Age-sensitive High Density Surface Electromyogram Indices for Detecting Muscle Fatigue Using Core Shape Modelling

Bharath Krishnan[1], Serena Zanelli[2,3], Sofiane Boudaoud[2], Léa Scapucciati[2], John McPhee[1], Ning Jiang[4*]

[1] Waterloo University, System Design Engineering, Waterloo, Canada

[2] Alliance Sorbonne University, Université de technologie de Compiègne, CNRS, UMR 7338 Biomechanics and Bioengineering, Centre de recherche de Royallieu, 60203 Compiegne cedex, France

[3]Politecnico Di Milano, Biomedical Engineering department, Milano, Italy

[4]National Clinical Research Center for Geriatrics， West China Hospital Sichuan University, and the Med-X Center for Manufacturing, Sichuan University, Chengdu, Sichuan Province, China

Keywords: *High density Electromyography; Aging; Muscle Fatigue; Core Shape Modelling, Gaussianity monitoring, Motor unit synchronization*

Abstract

The purpose of this preliminary study was to examine age-sensitive High Density surface Electromyogram (HD-sEMG) features by Core Shape Modelling (CSM) method. Fatiguing low force isometric contractions of the biceps brachii was performed by eight young (age, 24.40 ± 2.42 years) and five elderly (72.90 ± 2.21 years) males, while HD-sEMG recorded signals from the biceps brachii. The task was performed at 20% maximal voluntary contraction (MVC). From the recorded HD-sEMG signals, three Probability Density Function (PDF) shape distances (SD) measures the departure from Gaussianity, *i.e.* Left (LSD), Right (RSD), and Central (CSD), were derived by the CSM method from non-overlapping five-second windows until task failure. A linear regression analysis was then used to quantify the change of these shape parameters throughout the contraction. The resultant slopes revealed that the elderly group showed a decreasing trend in PDF shape parameters as the contraction approached task failure. In contrast, the young showed an

* Indicates the corresponding author: jiangning21@wchscu.cn

increasing trend. Statistical differences between the two groups were found for LSD (p=0.006) and RSD (p=0.001). No such age-sensitivity was detected using conventional sEMG fatigue features. These results suggest that the proposed CSM method can be used to obtain fatigue-related features from HD-sEMG that are age-sensitive and possibly related to different motor unit recruitment and synchronization schemes.

1. **Introduction**

Understanding physical limitations of the human body has been one of the primary focuses in the fields of sport, exercise, rehabilitation and ergonomics (Mori et al., 2016, Gu et al., 2018). Information about the underlying mechanisms responsible for these limitations are critical in the improvement of performance and/or prevention of musculoskeletal injury. One of the most prevalent mechanisms that results in a decrease in performance and increase in likelihood of injury is muscular fatigue, which can be defined as a decrease in maximum voluntary contraction force (MVC) or power production in response to contractile activity (Gandevia, 2001). Muscle fatigue is influenced by two systems and as such is typically split into the following categories: central fatigue and peripheral fatigue. Central fatigue stems from the central nervous system, which affects the neural drive to the motor neuron pool in a muscle leading to a reduction of force (Wan et al., 2017), whereas peripheral fatigue refers to the reduction of force generation capacity caused by skeletal muscle neurophysiological change (Cè et al., 2020).

It is accepted that advanced aging causes modifications to the neuromuscular system which can result in changes in the skeletal muscles such as their size, shape and fiber composition (Faulkner et al., 1995; Lexell, 1995). The abnormal age-associated loss of muscle mass and strength (force generation) is commonly referred to as sarcopenia. This condition typically results

* Indicates the corresponding author: jiangning21@wchscu.cn

in a loss of muscle fibers and an increase in fat infiltration at these sites (Santilli et al., 2014). Epidemiological studies show that the prevalence of sarcopenia increases from 5% from those aged 65-70 years old to 50% of those aged older than 80. Studies have shown that the prevalence of sarcopenia is expected to rise from 600 million in 2000 to 1.2 billion by 2025, costing upwards of 23.2 billion USD Although the relationship between changes in muscle mass and strength due to sarcopenia is well established (Brach & VanSwearingen, 2002; Faulkner et al., 1995), it is still not obvious how these factors affect the muscle resistance to fatigue.

To accurately model muscle fatigue using electrophysiological data, it is important to understand its underlying mechanisms. Typically, these mechanisms develop in the central and peripheral nervous system causing variations in motor unit (MU) recruitment strategies, conduction velocity or firing rate (McManus et al., 2016). Currently, Surface Electromyography (sEMG) is one of the most widely accepted non-invasive modalities used in capturing these variations (Cifrek et al., 2009). The sEMG signal typically depicts these changes in neuromuscular and morphological properties through modifications in its time-domain or spectral parameters and as such, these parameters are typically used to quantify muscle fatigue (Cifrek et al., 2009).

The robustness of these parameters in capturing age-related differences in fatigue development has been in question as of late. Although some studies exist that have found differences in these parameters with age (Yamada et al., 2000), several studies have not (da Silva et al., 2015; Habenicht et al., 2020; Yassierli et al., 2007) .The discrepancies in these results potentially indicates that age-related differences in fatigue development vary with contraction type, intensity and/or with muscle.

* Indicates the corresponding author: jiangning21@wchscu.cn

Apart from these well-established properties, motor unit synchronization has become progressively more relevant in recent literature concerning muscle fatigue. MU synchronization refers to the tendency of two MUs to fire within a fixed time interval with respect to each other, more frequently than chance (De Luca et al., 1993). In fact, recent studies have shown evidence that muscle fatigue had caused an increase in MU synchronization during sustained contraction (Beretta-Piccoli et al., 2015). A study that investigated the synchronization of MU activity during voluntary contraction revealed that the amount of synchronization reveals itself on a probabilistic level and is not apparent on visual inspection of the sEMG signal (Datta & Stephens, 1990). Considering this, a functional methodology, core shape modelling (CSM), explored by (S Boudaoud et al., 2010) investigated the modifications of the probability density function (PDF) shape during contraction due to MU synchronization. This methodology provided interesting results in classifying different levels of synchronicity and contraction intensity (Ayachi et al. 2014) on simulated sEMG signals. If synchronicity occurs during a fatiguing exercise, it induces modifications in the probability density shape: the more the MUs are synchronized the more likely for peaks and troughs to appear in the signals, leading to the modifications of the probability density function (S Boudaoud et al., 2010).

The primary aim of this study was to determine age-specific differences in measures derived from the CSM methodology between young and elderly males during fatiguing isometric contractions of the biceps brachii. Specifically, the effect of muscle fatigue on the shape of the HD-sEMG PDF was determined using Left (LSD), Right (RSD), and Central (CSD) shape distance measures derived from the CSM methodology. A secondary aim of this study was to compare this novel methodology to measures widely used in the literature such as time and frequency measures

* Indicates the corresponding author: jiangning21@wchscu.cn

from the sEMG signal, and torque variability measures extracted from force signals obtained from the dynamometer system (Al-Mulla et al., 2011; Tracy & Enoka, 2002). The HD-sEMG technique was used to record 64 sEMG signals from the biceps during contraction such that a Laplacian filter can be applied, to reduce the effect of crosstalk between the electrodes and to increase PDF shape modification contrast as observed in (Ayachi et al., 2014).

* Indicates the corresponding author: jiangning21@wchscu.cn

2. **Methods**

2.1. **Participants**

Twenty able-bodied male subjects were recruited from the University of Waterloo to participate in this study. Subjects were assigned to two groups based on their age; the young group consisted of 10 individuals between the ages of 22 and 30 years old (24.40 ± 2.42 years) and the elderly group had 8 males between the ages 68 and 75 years old (72.90 ± 2.21 years). All subjects were right-handed, and no one reported suffering from myopathy, abnormal pathologies, and musculoskeletal injury within the past six months. None of the participants required assistance for typical daily activities or had any cognitive impairments. Using the body mass index (BMI), no subject in either the young group (22.34±1.66) or the elderly group (25.55±3.06) was reported as underweight (BMI ≤ 18.5) or obese (BMI ≥ 30). Informed consent was obtained from each participant before the experiment and procedures were in accordance with the Declaration of Helsinki.

2.2. **Experimental Protocol**

A HD-sEMG electrode system (EMG-USB2+, OT Bioelettronica, Italy), was used to acquire sEMG data in monopolar montage. An 8x8 flexible electrode grid (10mm inter-electrode distance, 4mm electrode diameter) was placed on top of the biceps brachii (approximately placed between 20% and 61% of the upper limb length; Figure 1), with the reference electrode placed on the wrist after skin preparation. The signals recorded by the device were sampled at a rate of 2048 Hz, with a gain of 500.

* Indicates the corresponding author: jiangning21@wchscu.cn

A Dynamometer system (System 4 Pro, Biodex, USA) was used to acquire torque generated from the subject during exercise. This system ensured a fully isometric contraction as

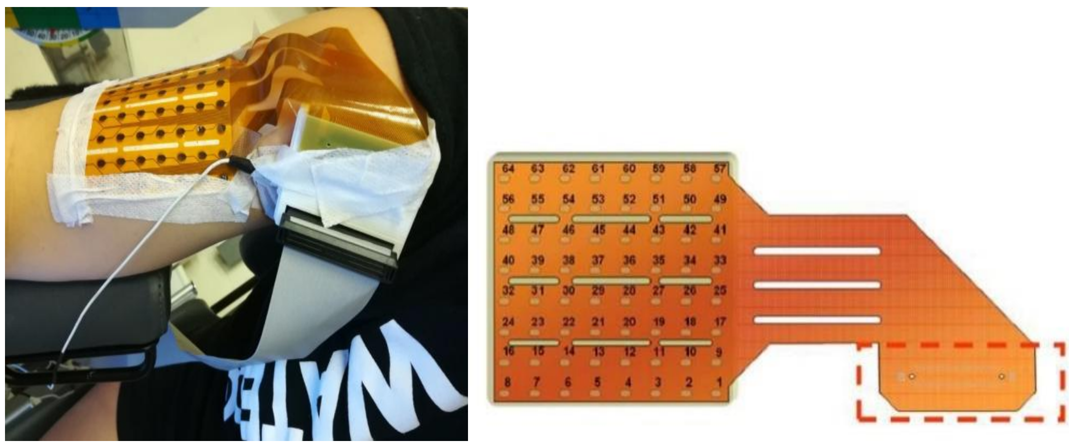

Figure 1: High Density sEMG (HD-sEMG) electrode grid placement on subject and numerical reference of the electrodes

zero velocity is maintained in all possible range of motions, allowing no significant variations in muscle length or joint angle during contraction. According to guidelines set by the manufacturer, the participants were seated in the dynamometer with 85° hip flexion from the anatomical position. The dynamometer arm was oriented 30° toward the participant which caused the forearm angle to be 30° from the horizontal prior to elbow flexion. Following calibration, the user was seated with their right elbow resting against a support. The forearm was placed in supination position firmly holding the fixed handle on the dynamometer arm. Due to the electrodes placed on the arm, it was not possible to immobilize the arm completely.

Before the experiment, the subject performed test contractions to get familiar with the experimental setup. During the experiment, both HD-sEMG and torque signals were recording continuously until the experiment was over. The subjects were first instructed to elicit a maximal voluntary contraction (MVC) by pulling the dynamometer handle towards them at maximal effort and maintaining it for five seconds. This was repeated three times to get an accurate reading of the

* Indicates the corresponding author: jiangning21@wchscu.cn

MVC value. To minimize the effect of fatigue on the MVC recordings, two-minute breaks were provided between the MVC contractions. Following the MVC contractions, subjects would rest for another two minutes. Then subjects were instructed to perform three brisk contractions to allow for realignment between the sEMG and torque data in offline analysis. Next, subjects were asked to maintain 20% MVC contraction until a subjectively determined endurance limit, which was defined as "task failure". Subjects were able to see their torque output overlaid with the 20% MVC target on a monitor, allowing them to constantly maintain a force above the 20% MVC torque objective.

2.3. **Data Processing**

The HD-sEMG signals recorded were filtered with a 4^{th} order Butterworth bandpass filter between 10 and 450Hz and then segmented into non-overlapping 5-second analysis windows. Power-line interference was rejected through a feedback circuit located on the amplifier within the HD-sEMG electrode system. An expert inspected the raw HD-sEMG data for quality assurance, identifying channels that either have no signal or excessive noise (<1% of the channels recorded, only found in five subjects). The data of these channels were substituted by the average value of surrounding channels. As task failure was subjectively determined by each participant, the presence of fatigue was confirmed through an increase rate in average rectified value (ARV) throughout the contraction. Participants that did not exhibit an increasing trend were excluded. The signal-to-noise ratio (SNR) for each subject was calculated to eliminate participants that had noisy EMG signals. This metric represents the ratio of the EMG signal during a contraction over the background noise during the resting periods. The SNR for each recording was calculated using a one second non-overlapping moving window and translating it over the duration of the entire signal. The noise was then determined by taking a one second window of the two-minute rest

* Indicates the corresponding author: jiangning21@wchscu.cn

periods in-between MVC contractions at the beginning of the protocol. Signals with excessive noise (mean SNR<12dB over the 64 channels) were excluded from the study. This resulted in 8 young and 5 elderly subjects to remain for further analysis.

Signals that are recorded using the monopolar configuration are highly susceptible to crosstalk contamination. To mitigate the effects of this, spatial filters such as the Laplacian filter are introduced, as explained in the **2.6** subsection. Following the segmentation of the signal into nonoverlapping 5 second windows, the sEMG features, including average rectified value (ARV), mean frequency (MNF), and median frequency (MDF) were extracted. In addition, PDF shape analysis features, including left shape distance (LSD), right shape distance (RSD) and central shape distance (CSD), were extracted as well. The details of these shape analysis features are presented below in subsection **2.5**. Using the data from the three brisk contractions taken before the fatiguing contractions, an alignment procedure was employed to realign the EMG and torque signals. First, the cross-correlation function between the HD-sEMG signals and the torque signal of the three brisk contractions was calculated. Next, the position of the peak values of the cross-correlation function was identified, which is subsequently used to realign the HD-sEMG signals and the torque properly.

2.4. **Torque Analysis**

The ability to produce consistent torque while performing a task is known to decline with age (Tracy & Enoka, 2002). As such, the coefficient of variation (CV) was selected to quantify the consistency of the torque throughout the fatiguing contraction for both groups. This was performed by segmenting the acquired torque signal, from the start of the contraction to failure, into non-overlapping 5-second segments. The CV was then calculated for each of these segments for the entire length of the torque signal.

* Indicates the corresponding author: jiangning21@wchscu.cn

2.5. **Shape Analysis**

Core shape modelling (CSM) is a shape analysis technique that provides an average shape curve and distance measure of shapes that can be used to describe shape dispersion among a set of signals. For the polynomial degree of k=1, the average shape curve (formally known as core shape) is invariant to any linear time transforms, which allows for the conservation of shape (S. Boudaoud et al., 2010). The CSM approach has been successfully used to measure the distance of simulated sEMG with non-Gaussian PDF shapes (S. Boudaoud et al., 2014, Ayachi et al., 2014) and in monitoring P-wave modifications with sleep apnea (Boudaoud et al., 2007). These metrics were used as an evaluation criterion in the current study. To generate a core shape (CS) model, a set of N time series s_i positive on their time support and linked in the normalized integral domain F is considered and expressed as:

$$S_i = \Gamma_{cs} \circ \varphi_i \tag{1}$$

where S_i is the normalized integral of the s_i time series, Γ_{cs} is the normalized integral of the CS curve and the φ_i function represents the shape and time variability. $S_i = \Gamma_{cs} \circ \varphi_i$ is shorthand notation for the composition function $S_i = \Gamma_{cs}(\varphi_i(x))$. Suppose that $p(x)$ and $g(x)$ are probability density functions (PDFs) that depict a random sEMG PDF and a Gaussian PDF, respectively. The normalized integrals $p(x)$ and $g(x)$ can be represented using the following equations (S. Boudaoud et al., 2014):

$$P(x) = \frac{\int_{a_p}^{x} p(u)du}{\int_{a_p}^{b_p} p(u)du}, G(x) = \frac{\int_{a_g}^{x} g(u)du}{\int_{a_g}^{b_g} g(u)du} \tag{2}$$

where $[a_p,b_p] \subset [-1,1]$, $[a_g,b_g] \subset [-1,1]$ are the nonzero supports of $p(x)$ and $g(x)$, respectively. Using the relationship stated in (1) the distribution functions $P(x)$ and $G(x)$ can be connected using a warping function, φ or ψ:

* Indicates the corresponding author: jiangning21@wchscu.cn

$$P(x) = G(x)\circ\varphi_i \;, G(x) = P(x)\circ\psi_i \tag{3}$$

where the time warping function $\psi = \varphi^{-1}$ links both distribution functions and represents the fluctuations of the CS curve in both shape and abscissa support (S. Boudaoud et al., 2010). For an accurate PDF analysis, it is important to isolate intrinsic shape variations from variations caused by first or second order moments. To do this, the warping function is proposed in the following way:

$$\varphi_i = v \circ A(x),\; \psi_i = A^{-1}(x) \circ w\,,\; w = v^{-1} \tag{4}$$

where A is defined as affine polynomial function that accounts the for mean and variance of $p(x)$ and is represented by the function $A(x) = \alpha x + \beta$. Using this relationship, (4) can be written as follows in the F and F^{-1} respectively (Sofiane Boudaoud et al., 2007).

$$P(x) = G(x)\circ v \circ A(x)\,,\; G(x) = P(x)\circ A^{-1}(x) \circ w$$
$$P^{-1}(x) = G^{-1}(x)\circ w \circ A^{-1}(x)\;, A(x) \circ P^{-1}(x) = G^{-1}(x) \circ w \tag{5}$$

In this context, w, and v, are increasing nonlinear functions that characterize shape fluctuation present on the same time support in the CS and can be written as:

$$w_i(y) = n_i(y) + y\,,\; v_i(y) = m_i(y) + y \tag{6}$$

The functions $n_i(y)$ and $m_i(y)$ characterize the amount of intrinsic shape fluctuations present in the set of curves. Therefore, by rewriting (5) and substituting this equation into the rewritten form, a function can be derived and simplified as:

$$\alpha P^{-1}(y) + \beta = G^{-1}(y) + n_i\big(G^{-1}(y)\big),\; y \in [0,1] \tag{7}$$

where $n_i(G^{-1}(y))$ is the shape difference between the realigned function $\hat{A}(P^{-1}(y))$ and $G^{-1}(y)$. The α and β values are approximated using a constrained linear regression between $P^{-1}(x)$ and $G^{-1}(x)$. Using this, three distances, the Center Shape Distance (CSD), that evaluates PDF peakedness, the Left Shape Distance (LSD) and the Right Shape Distance (RSD), that both evaluate PDF

* Indicates the corresponding author: jiangning21@wchscu.cn

assymetry, are proposed to quantify the shape differences between the realigned function and $\hat{A}(P^{-1}(y))$ and $G^{-1}(y)$. These distances exhibited robustness against noise and small sample effect compared to classical high order statistics (S. Boudaoud et al. 2014). They are defined as follows for two PDFs p, q in the continuous domain (numerical expression are available):

$$CSD_{(p,q)} = \sqrt{\int_{0.4}^{0.6} \left(\alpha P^{-1}(y) + \beta - G^{-1}(y)\right)^2 \mathrm{d}y} \tag{8}$$

$$LSD_{(p,q)} = \sqrt{\int_{0}^{0.25} \left(\alpha P^{-1}(y) + \beta - G^{-1}(y)\right)^2 \mathrm{d}y} \tag{9}$$

$$RSD_{(p,q)} = \sqrt{\int_{0.75}^{1} \left(\alpha P^{-1}(y) + \beta - G^{-1}(y)\right)^2 \mathrm{d}y} \tag{10}$$

2.6. **EMG Spatial Filtering**

The 64-channel electrode grid allowed spatial filtering to allow better spatial resolution. In this study, a classic Laplacian spatial filter was used. It is a spatially high-pass filter and is more sensitive to the activities of the superficial motor units of the muscle directly below the measurement site (Fukuoka et al., 2013). As such, it is also less susceptible to surface EMG crosstalk (Fukuoka et al., 2013). It has been also observed that Laplacian filtering increases PDF shape changes in sEMG signals related to MU control scheme modifications (Ayachi et al. 2014).

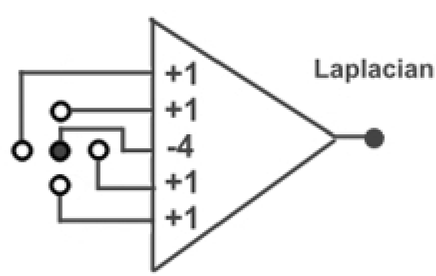

Figure 2: Laplacian Configuration of Electrodes in HD-sEMG

* Indicates the corresponding author: jiangning21@wchscu.cn

The Laplacian filter is set up by assigning fixed weighting factors (see Figure 2) to one electrode and other electrodes surrounding it, and the output of the filter is the weighted summation of all the channels, i.e. one virtual sEMG signal. In the current study, a Laplacian configuration was used and moved over the grid. Thus, 36 Laplacian channels were obtained from the 64 monopolar ones.

2.7. HD-sEMG Feature Extraction

For assessing muscular fatigue, three widely used features were extracted from the HD-sEMG signal after Laplacian filtering. In the time domain, the average rectified value (ARV) was used to characterize the amplitude, which helped give insight into the muscle activities under fatiguing conditions (Al-Mulla et al., 2011). The ARV was calculated by using the following discrete equation:

$$\mathrm{ARV} = \frac{1}{N_{tot}} \sum_{i=1}^{N_{tot}} |x_i| \tag{11}$$

where N_{tot} is the number of samples chosen in the time window, and x_i is the i th sample of the analyzed sEMG signal. In the frequency domain, the mean frequency (MNF) and median frequency (MDF), from power spectral density (PSD) estimated by Welch method, was used to represent the sEMG spectral component during fatiguing contractions. Indeed, they are known to reflect the muscle fiber conduction velocity (Merletti et al., 1990a). For both spectral indices, every five second window of the sEMG signal throughout the fatiguing contraction was further split into five smaller time-windows. For each window within the five sub-windows the periodogram has been estimated and then averaged over the five sub-windows. The following discrete expressions were used to calculate the mean frequency and median frequencies:

* Indicates the corresponding author: jiangning21@wchscu.cn

$$MNF = \frac{\sum_{k=1}^{F_{tot}} f_k \, S_k}{\sum_{k=1}^{F_{tot}} S_k} \tag{12}$$

$$\sum_{k=1}^{MDF} S_k = \sum_{k=MDF}^{F_{tot}} S_k \tag{13}$$

where F_{Tot} is the total frequency bins and S_k is the magnitude of the power spectrum at the kth bin.

Using the CSM approach presented in section **2.5**, the effect of muscular fatigue was analyzed by generating a PDF of the spatially filtered sEMG signal. For this, the Gaussian curve is used as a reference and the PDF of the sEMG signal was estimated by a kernel density estimator. The LSD, RSD and CSD shape parameters extracted from the CSM were charted throughout the protocol and the trend of each parameter was investigated throughout the entire time course of the signal. Similarly, the time/spectral parameters were tracked throughout the protocol to observe how to accumulation of fatigue affects each parameter, as commonly seen in the literature (Cifrek et al., 2009; Georgakis et al., 2003).

2.8. Statistical Analysis

For each of the young and elderly groups, the trend of the ARV, MDF and MNF parameters were calculated using a linear regression to observe any differences in the trend of each parameter. Mann-Whitney U tests were employed to investigate whether they varied significantly across both age groups in the study. The shape distances extracted through shape analysis were calculated from Laplacian HD-sEMG signals and averaged over the 36 channels. To compare the effect each state had on the three shape distances, a linear regression was performed to investigate the change of each shape parameter during the fatigue protocol. The slopes derived from the regression analysis was then averaged for each group and a Mann-Whitney U test was used to test for significance. For all analyses, the level of significance was set to 0.05.

* Indicates the corresponding author: jiangning21@wchscu.cn

* Indicates the corresponding author: jiangning21@wchscu.cn

3. **Results**

3.1. **Torque Analysis**

The coefficient of variation (CV) of the torque was charted in 5 second bins throughout the entirety of the recorded signal for both young and elderly groups, as seen in Figure 3A and 3C.Within each group, a linear regression revealed that the CV generally increased as the contraction approached fatigue, which is consistent with the literature (Hunter et al., 2005; Ng et al., 2003). However, the observed change was not significant within either group when comparing CV at the start of the contraction and just before task failure, as seen in Figure 3D. The Mann-

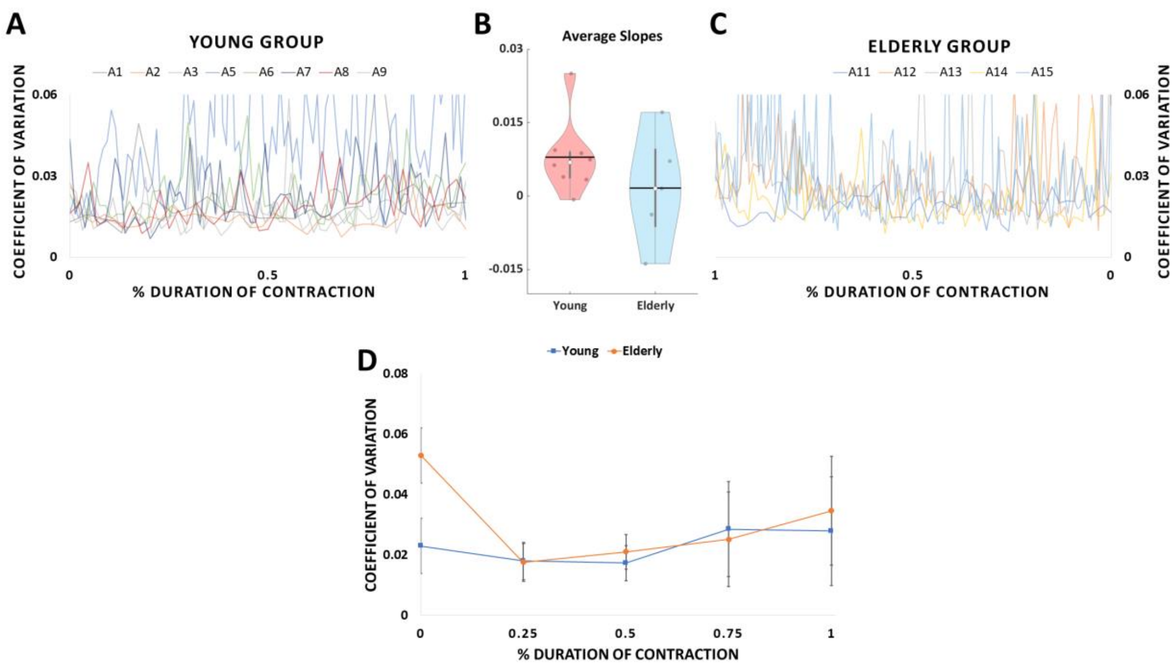

Figure 3: Coefficient of Variation (CV) values calculated in 5 second bins along a normalized time axis for each subject, with (A) being the young group and (C) being the elderly group. (B) Violin plot depicting the distribution of CV slopes derived from Linear Regression analysis of subjects throughout the length of the contraction. (D) Fluctuations in torque quantified as the coefficient of variation (CV) for the torque exerted by the biceps. Mean (±SD) CV of the torque is shown for young and elderly men for 5-s intervals at the start, 25,50,75 and 100% of the time the sustained contraction reached task failure.

Whitney U test revealed that there was no significant difference in CV between the beginning of the contraction and just before failure in the young (p=0.1949) and elderly (p=0.4206) groups. Comparison of the average CV between both groups at the beginning (p=0.0655) and before failure

* Indicates the corresponding author: jiangning21@wchscu.cn

(p=0.3054) also revealed no significant difference. The slopes of the trend lines calculated using linear regression, are shown using violin plots in Figure 3B (Bechtold, 2016). This revealed that the young group had a higher average slope of 0.007 ± 0.007 when compared to the elderly group which had a slope of 0.001 ± 0.013. Although the young group was higher, there was no significant difference between the CV slopes of both groups (*p*=0.2844).

3.2. **Time and Frequency Analysis**

The Figure 4 shows the rate of change of the ARV, MNF, and MDF parameters throughout the contraction. In general, ARV parameter increased in the fatiguing conditions, while MNF and MDF parameters decreased, which is expected and in agreement with other reports in the literature (Cifrek et al., 2009; Daanen et al., 1990; Merletti et al., 1990b).

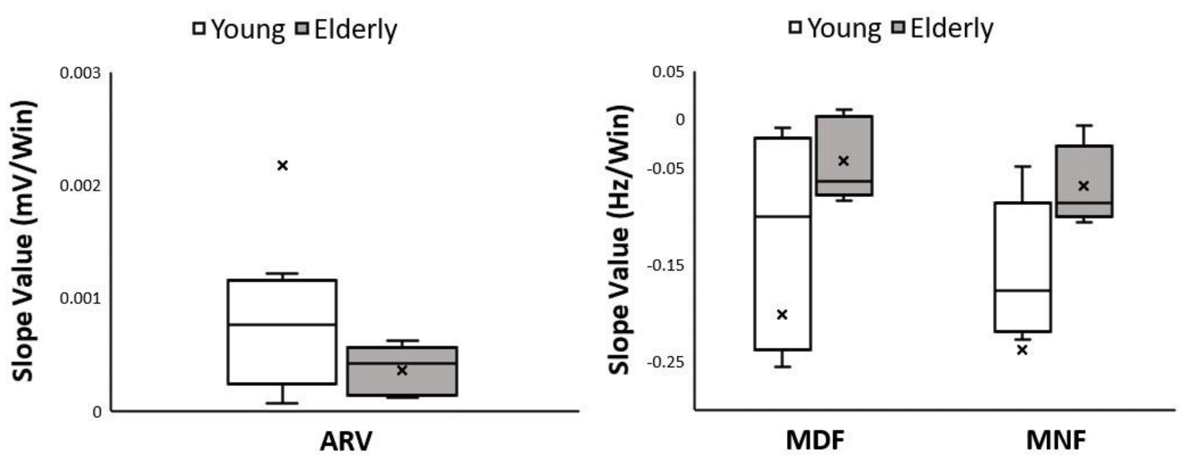

Figure 4: Boxplot of the slopes extracted from the linear regression of the conventional sEMG features, i.e., ARV, MDF and MNF and non-overlapping 5 windows (Win) throughout the fatiguing contraction for young (white) and elderly (grey) subjects. The mean of each group is shown through the 'x' marker.

More interestingly, the two frequency domain indices (MNF and MDF) showed slightly larger changes in young population than in the elderly group. The median MNF and MDF of the young population decreased at a rate of -0.101Hz/Win and -0.176Hz/Win respectively as the

* Indicates the corresponding author: jiangning21@wchscu.cn

contraction reached mechanical failure. The elderly population only decreased -0.063Hz/Win and -0.086Hz/Win for the same indices. No meaningful difference was found in ARV, with the ARV increasing -0.757μV/Win for the young group and the elderly group increasing at a lesser rate of -0.422μV/Win .However, due to large variability in the data, Mann-Whitney U tests between both groups reported non-significant changes for the time domain feature ARV (*p*=0.127) as well as frequency domain features MDF (*p*=0.435) and MNF (*p*=0.354).

3.3. **Shape Analysis**

The PDF shape distances throughout the contraction, between the different populations (young and elderly) were quantified using the LSD, RSD and CSD shape parameters. Shape parameter analysis revealed that the elderly group exhibited different changes in average shape parameter values during sustained contraction when compared to the young group. This was quantified using a linear regression which computed the average shape parameter, for each subject with respect to

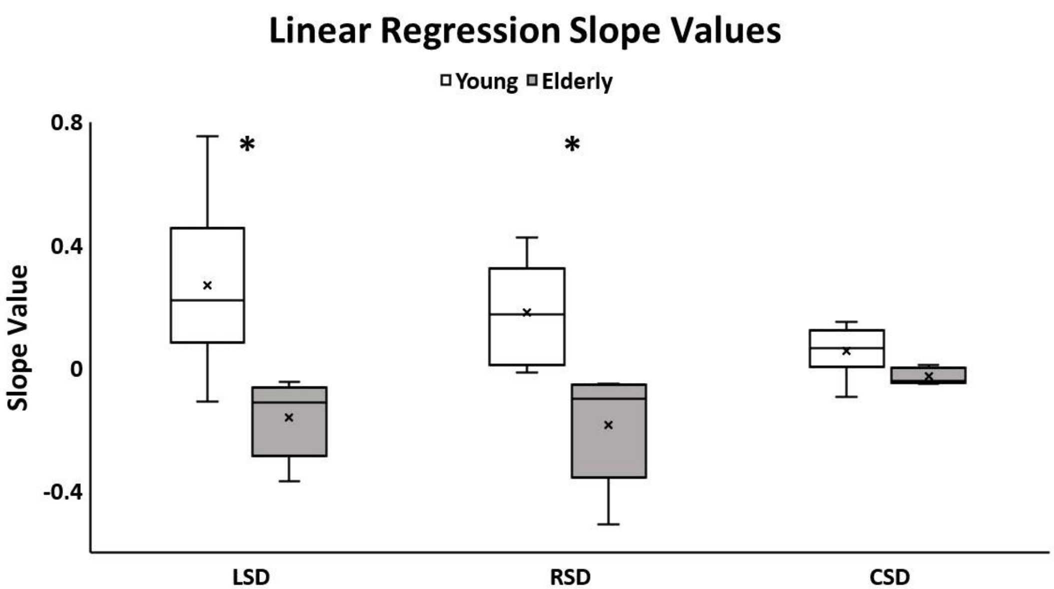

*Figure 5: Average slope value (derived from linear regression) of each shape parameter (LSD, RSD, CSD) calculated from the start of the contraction to task failure. This is shown for both young (white) and elderly (black) groups. * Indicates significant differences (p<0.05) between both groups.*

* Indicates the corresponding author: jiangning21@wchscu.cn

the time axis normalized to the length of the sustained contraction, as shown in Figure 5**Error! Reference source not found.** and Figure 6.

Interestingly, within the young group, all shape parameters displayed positive slope values, with the LSD shape parameter increasing the most with an average slope of 0.268 ± 0.256. The RSD and CSD shape parameters increased at a slightly slower rate with average slopes of 0.176± 0.154 and 0.053± 0.074, respectively. In contrast, the elderly group results showed that the shape parameters generally decreased as the contraction went on. The RSD parameter decreased at the most rapid rate with a slope of -0.185± 0.171, while LSD and CSD parameters decreased moderately with slopes of -0.162± 0.115 and -0.028± 0.024, respectively. Mann-Whitney U test revealed that there was a significant difference for the LSD (p=0.006) and RSD (p=0.001) shape

* Indicates the corresponding author: jiangning21@wchscu.cn

parameter slopes between both groups and non-significant differences in CSD (p=0.065). This change in shape parameters as subjects approach failure in both young and elderly groups are depicted in Figure 6.

4. Discussion

The primary goal of this preliminary study was to compare differences in muscle fatigue development of the biceps brachii for young and elderly males during sustained low effort (20% MVC) contractions. Widely used torque and sEMG parameters in the detection of muscle fatigue

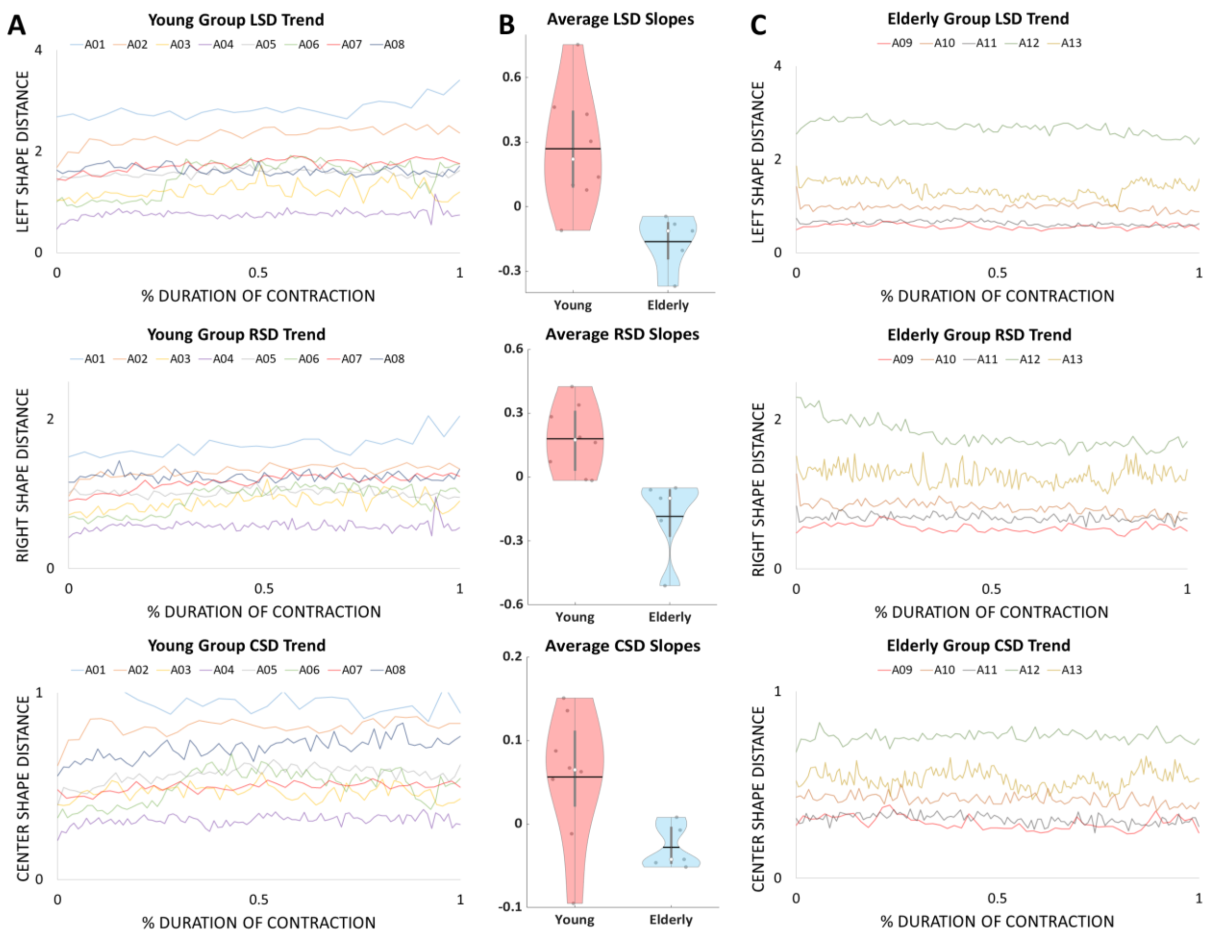

Figure 6: Shape parameters extracted from experimental data recorded using Laplacian configuration during sustained fatiguing contraction. Column A, Shape parameters, from top to bottom, left shape distance (LSD); right shape distance (RSD); center shape distance (CSD) calculated from the beginning of the contraction (0) to failure (1) for the young group. Column C, from top to bottom: Shape parameters calculated for the elderly group. Column B depicts the average slopes of each shape parameter derived from linear regression analysis of subjects throughout the length of the contraction.

* Indicates the corresponding author: jiangning21@wchscu.cn

were employed, discovering no difference in fatigue development between young and elderly groups. As a result, one can conclude that these parameters may not be robust enough to capture these age-related differences. Using the described CSM formalism, shape distance parameters (LSD, RSD and CSD) were able to distinguish between the age groups. The new findings indicate that there was an increase in the LSD and RSD parameters in the young group as the contraction reached failure. In contrast, the elderly group displayed a decreasing trend for the same parameters. Thus, it appears that contribution of MU synchronization, as characterized by increasing shape parameter values, related to a departure from Gaussianity, was increased in the young group as muscle fatigue developed (see next section for details).

A section of this study was designed to investigate the variability of torque throughout the entire length of the bicep sustained contraction task in both young and elderly males. Linear regression analysis revealed that torque variability was not significantly different between both groups (Figure 3). Many studies have investigated the effect that age has on the variability of torque while producing consistent, submaximal isometric torques (Galganski et al., 1993; Laidlaw et al., 2000; Tracy & Enoka, 2002). These studies typically evaluate the torque variability using either the coefficient of variation or standard deviation of the torque signal. The results found in this study are generally consistent with the literature, with the elderly group having higher force fluctuations throughout the sustained contraction. At the start of the contraction, the elderly group had higher magnitudes of fluctuations, which has also been seen in other studies. This behavior could stem from a more variable discharge rate resulting from aged active motor units (Hunter et al., 2005; Laidlaw et al., 2000; Tracy et al., 2005). Linear regression analysis revealed that the young group had a more rapid increase in torque fluctuations as the contraction continues toward

* Indicates the corresponding author: jiangning21@wchscu.cn

fatigue when compared to the elderly group. This is likely due to a more rapid rate of recruitment of motor units that have increased discharge rate variability during the fatiguing task (Hunter et al., 2005; Moritz et al., 2005). Though these changes were consistent with the literature, the changes were not statistically significant between both groups, suggesting that this metric is not sensitive enough to capture age-related differences in fatigue development.

4.1. **PDF Shape Parameter Slope Differences between Young and Elderly groups**

To find a more robust methodology to assess age-related differences in muscle fatigue development, the CSM approach was adopted, and shape parameters were extracted from the HD-sEMG amplitude PDF after Laplacian filtering. The analysis results revealed that all shape parameters in the young group increased as the contraction approached mechanical failure. On the contrary, all shape parameters in the old group decreased, with LSD and RSD parameters being significantly different from the young group. This behavior suggested that the elderly group relied less on MU synchronization as the PDFs of the Laplacian HD-sEMG signal became more Gaussian as the contraction approached mechanical failure. Conversely, the increasing shape parameters for the young population suggest that there is likely an increase in MU synchronization. This behavior in young subjects is also consistent with another study that investigated MU synchronization and muscle fatigue at low (20-30% MVC) contraction levels (Holtermann et al., 2009).

The differences in the MU synchronization between both groups contrasts with a previous study, which adopted much higher levels of contraction (70% MVC). It was shown that the elderly group displayed more MU synchronization than the young group (Boccia et al., 2015). The discrepancies in the results could be attributed to how the neuromuscular physiology of the aged muscle reacts to differing contraction levels. With aging, it is well known that the number and size of type II (fast) MUs are reduced and remaining MUs have higher innervation ratios (Wu et al.,

* Indicates the corresponding author: jiangning21@wchscu.cn

2020). This can potentially result in aged muscle reacting differently during sustained contractions of varying intensities. This is evidenced by the fact that higher contraction forces typically use a considerable amount of type II MUs in order to sustain the contraction (Sale, 1987). Considering this, it can be postulated that the remaining type II MUs increase in synchrony to sustain the higher contraction forces. Aged MUs are known to innervate more muscle fibers of the slow twitch type (Campbell et al., 1973), potentially making it more efficient at sustaining lower force contractions thus causing a reduction in MU synchronization. However, this has yet to be validated in the literature thus warranting additional studies on the effect of contraction intensity on MU synchronization in the elderly.

The differences in MU synchronization and recruitment between both age groups can be attributed to different MU type distributions within the muscle anatomy of young and elderly subjects. When comparing the MU distribution in the Biceps Brachii of both groups, the elderly exhibited a lower number and size of type II MUs (Klein C.S et al. 2003). This can lead to modified synchronization and recruitment strategy during fatigue development. This suggests that the aged muscle can rely more on resistant type I (slow) MUs when compared to young muscle that has more type II MUs that are more fatigable and perhaps more solicited during long sustained contractions even at low-level isometric contraction level explaining increased torque CV slopes for young subjects compared to elder ones (see Figure 6). This should have a strong impact on the MU recruitment and synchronization scheme during fatigue and can explain the significant differences observed in this study. In fact, increasing recruitment of type II (rapid) superficial MUs, combined with specific synchronization strategies and better Laplacian detection, can explain the positive slope observed in the young category due to increased non-Gaussianity

* Indicates the corresponding author: jiangning21@wchscu.cn

behavior. In contrary, older subjects seem to recruit deeper type I (slow) MUs and less type II (rapid) MUs, as supposed before, with less synchronization and different recruitment scheme that can explain a return to Gaussianity toward task failure, and the observed negative slope.

A recent simulation study has demonstrated the impact of MU type distribution on the PDF shape distance trends from HD-sEMG signals with varying contraction level but with not varying synchronization using a multiscale neuromuscular model (M. Al Harrach et al. 2017). However, a direct link has been demonstrated, in simulation, between the level of MU synchronization and PDF shape modifications (departure from Gaussianity) of sEMG signals using CSM formalism (S. Boudaoud et al., 2010). Thus, specific fatigue simulation scenario, using recent neuromuscular modelling (Carriou et al 2018), are definitively needed to test the proposed hypotheses, namely, type dependent MU recruitment scheme and synchronization, occurring during fatigue in future studies.

4.2. **Implications**

The results from the current study agreed with the existing evidence that MU synchronization is a significant factor in the development of muscle fatigue (Dartnall et al., 2008). This experiment also provides new insight into the difference of MU synchronization and recruitment in the fatigue development between young and elderly age groups. Thus, shape parameters revealed that the younger group seems to exhibit increasing level of MU synchronization as the low-level contraction approached failure, while the elderly group showed decreasing level. This antagonist behavior with aging cannot be related to simple well-known conduction velocity decrease with fatigue. This showcases that the proposed PDF shape analysis methodology is more sensitive to fatigue-related functional changes in elderly people when compared to conventional approaches, such as torque analysis and conventional sEMG features in

* Indicates the corresponding author: jiangning21@wchscu.cn

time and frequency domain. As such, the proposed methodology provides insight into neuromuscular changes such as motor unit synchronization and distinguishes between different age groups during fatiguing contractions. In this study, indices averaging over the grid has been favored. This choice is justified for providing simple, robust and comprehensive metrics for the next clinical studies with larger cohorts. Thus, the proposed scalar indices simplify the statistical comparative study to measure aging effect on muscle fatigue. Naturally, further studies are planned to better assess the spatial repartition of PDF deformations over the HD-sEMG grid, measured by shape CSM formalism, with fatigue and aging in a near future.

4.3. **Limitations**

A key limitation to this study is the relatively small size of the studied cohort. Multiple reasons exist for the excess exclusion of elderly males such as increased subcutaneous fat in the arm regions, adversely affecting the sEMG signal quality. Another limitation is that we were unable to distinguish if the elderly participants were undergoing fatiguing contractions. As the user was told to go until failure, there is some uncertainty in how each user perceives failure. This is especially noticed in elderly participants as spectral analysis revealed positive trends in their MDF meaning that they perceive failure before their muscles fatigue. Future studies will focus on the recruitment of larger cohorts and will develop procedures to ensure that they truly exhibit muscle fatigue. The gender effect and possible relationship with muscle atrophy was also not investigated in the study and should be included in future studies.

* Indicates the corresponding author: jiangning21@wchscu.cn

5. **References**

Al Harrach, M, Boudaoud, S, Carriou, V, Laforet, J, Letocart, A, Grosset, J.F., Marin, F.(2017) Investigation of the HD-sEMG probability density function shapes with varying muscle force using data fusion and shape descriptors. *Comput. in Biol. & Med.*. 89:44-58. DOI: 10.1016/j.compbiomed.2017.07.023. PMID: 28783537.

Ayachi, F. S, Boudaoud, S, & Marque, C. (2014). Evaluation of muscle force classification using shape analysis of the sEMG probability density function: a simulation study. *Med Biol Eng Comput.* 52, pages 673–684. https://doi.org/10.1007/s11517-014-1170-x

Al-Mulla, M. R., Sepulveda, F., & Colley, M. (2011). A review of non-invasive techniques to detect and predict localised muscle fatigue. *Sensors*, *11*(4), 3545–3594. https://doi.org/10.3390/s110403545

Bechtold, B. (2016). *Violin Plots for Matlab*. Github Project. https://doi.org/10.5281/zenodo.4559847

Beretta-Piccoli, M., D'Antona, G., Barbero, M., Fisher, B., Dieli-Conwright, C. M., Clijsen, R., & Cescon, C. (2015). Evaluation of central and peripheral fatigue in the quadriceps using fractal dimension and conduction velocity in young females. *PloS One*, *10*(4), e0123921. https://doi.org/10.1371/journal.pone.0123921

Boccia, G., Dardanello, D., Beretta-Piccoli, M., Cescon, C., Coratella, G., Rinaldo, N., Barbero, M., Lanza, M., Schena, F., & Rainoldi, A. (2015). Muscle fiber conduction velocity and fractal dimension of EMG during fatiguing contraction of young and elderly active men. *Physiological Measurement*, *37*(1), 162–174. https://doi.org/10.1088/0967-3334/37/1/162

Boudaoud, S., Rix, H., Harrach, M. Al, & Marin, F. (2014). Robust functional statistics applied to probability density function shape screening of sEMG data. *2014 36th Annual International Conference of the IEEE Engineering in Medicine and Biology Society, EMBC 2014*, *1*, 2213–2216. https://doi.org/10.1109/EMBC.2014.6944058

Boudaoud, S., Rix, H., & Meste, O. (2010). Core Shape modelling of a set of curves. *Computational Statistics and Data Analysis*, *54*(2), 308–325. https://doi.org/10.1016/j.csda.2009.08.003

Boudaoud, S, Ayachi, F., & Marque, C. (2010). Shape analysis and clustering of Surface EMG Data. *2010 Annual International Conference of the IEEE Engineering in Medicine and Biology*, 4703–4706. https://doi.org/10.1109/IEMBS.2010.5626378

Boudaoud, Sofiane, Rix, H., Meste, O., Heneghan, C., & O'Brien, C. (2007). Corrected Integral Shape Averaging Applied to Obstructive Sleep Apnea Detection from the Electrocardiogram. *EURASIP Journal on Advances in Signal Processing*, *2007*. https://doi.org/10.1155/2007/32570

Brach, J. S., & VanSwearingen, J. M. (2002). Physical impairment and disability: relationship to performance of activities of daily living in community-dwelling older men. *Physical Therapy*, *82*(8), 752–761.

* Indicates the corresponding author: jiangning21@wchscu.cn

Campbell, M. J., McComas, A. J., & Petito, F. (1973). Physiological changes in ageing muscles. *Journal of Neurology, Neurosurgery, and Psychiatry*, *36*(2), 174–182. https://doi.org/10.1136/jnnp.36.2.174

Carriou, V., Boudaoud, S. & Laforet, J (2018). Speedup computation of HD-sEMG signals using a motor unit-specific electrical source model. Medical & Biological Engineering & Computing, Volume 56, Issue 8, pp 1459–1473

Cè, E., Longo, S., Limonta, E., Coratella, G., Rampichini, S., & Esposito, F. (2020). Peripheral fatigue: new mechanistic insights from recent technologies. *European Journal of Applied Physiology*, *120*(1), 17–39. https://doi.org/10.1007/s00421-019-04264-w

Cifrek, M., Medved, V., Tonkovic, S., & Ostojić, S. (2009). Surface EMG Based Muscle Fatigue Evaluation in Biomechanics. *Clinical Biomechanics (Bristol, Avon)*, *24*, 327–340. https://doi.org/10.1016/j.clinbiomech.2009.01.010

da Silva, R. A., Vieira, E. R., Cabrera, M., Altimari, L. R., Aguiar, A. F., Nowotny, A. H., Carvalho, A. F., & Oliveira, M. R. (2015). Back muscle fatigue of younger and older adults with and without chronic low back pain using two protocols: A case-control study. *Journal of Electromyography and Kinesiology : Official Journal of the International Society of Electrophysiological Kinesiology*, *25*(6), 928–936. https://doi.org/10.1016/j.jelekin.2015.10.003

Daanen, H., Mazure, M., Holewijn, M., & Velde, E. (1990). Reproducibility of the mean power frequency of the surface electromyogram. *European Journal of Applied Physiology and Occupational Physiology*, *61*, 274–277. https://doi.org/10.1007/BF00357612

Dartnall, T. J., Nordstrom, M. A., & Semmler, J. G. (2008). Motor unit synchronization is increased in biceps brachii after exercise-induced damage to elbow flexor muscles. *Journal of Neurophysiology*, *99*(2), 1008–1019. https://doi.org/10.1152/jn.00686.2007

Datta, A. K., & Stephens, J. A. (1990). Synchronization of motor unit activity during voluntary contraction in man. *The Journal of Physiology*, *422*, 397–419. https://doi.org/10.1113/jphysiol.1990.sp017991

De Luca, C. J., Roy, A. M., & Erim, Z. (1993). Synchronization of motor-unit firings in several human muscles. *Journal of Neurophysiology*, *70*(5), 2010–2023. https://doi.org/10.1152/jn.1993.70.5.2010

Faulkner, J. A., Brooks, S. V, & Zerba, E. (1995). Muscle atrophy and weakness with aging: contraction-induced injury as an underlying mechanism. *The Journals of Gerontology. Series A, Biological Sciences and Medical Sciences*, *50 Spec No*, 124–129. https://doi.org/10.1093/gerona/50a.special_issue.124

Fukuoka, Y., Miyazawa, K., Mori, H., Miyagi, M., Nishida, M., Horiuchi, Y., Ichikawa, A., Hoshino, H., Noshiro, M., & Ueno, A. (2013). Development of a Compact Wireless Laplacian Electrode Module for Electromyograms and Its Human Interface Applications. In *Sensors* (Vol. 13, Issue 2). https://doi.org/10.3390/s130202368

* Indicates the corresponding author: jiangning21@wchscu.cn

Galganski, M., Fuglevand, A., & Enoka, R. (1993). Reduced control of motor output in a human hand muscle of elderly subjects during submaximal contractions. *Journal of Neurophysiology*, *69*, 2108–2115. https://doi.org/10.1152/jn.1993.69.6.2108

Gandevia, S. (2001). Spinal and Supraspinal Factors in Human Muscle Fatigue. *Physiological Reviews*, *81*, 1725–1789. https://doi.org/10.1152/physrev.2001.81.4.1725

Georgakis, A., Stergioulas, L. K., & Giakas, G. (2003). Fatigue analysis of the surface EMG signal in isometric constant force contractions using the averaged instantaneous frequency. *IEEE Transactions on Bio-Medical Engineering*, *50*(2), 262–265. https://doi.org/10.1109/TBME.2002.807641

Gu, Y., Yang, D., Huang, Q., Yang, W., and Liu, H. (2018). Robust EMG pattern recognition in the presence of confounding factors: features, classifiers and adaptive learning. *Expert Systems With Applications*, 96, 208-217. https://doi.org/10.1016/j.eswa.2017.11.049

Habenicht, R., Ebenbichler, G., Bonato, P., Kollmitzer, J., Ziegelbecker, S., Unterlerchner, L., Mair, P., & Kienbacher, T. (2020). Age-specific differences in the time-frequency representation of surface electromyographic data recorded during a submaximal cyclic back extension exercise: a promising biomarker to detect early signs of sarcopenia. *Journal of NeuroEngineering and Rehabilitation*, *17*(1), 8. https://doi.org/10.1186/s12984-020-0645-2

Holtermann, A., Grönlund, C., Karlsson, J. S., & Roeleveld, K. (2009). Motor unit synchronization during fatigue: Described with a novel sEMG method based on large motor unit samples. *Journal of Electromyography and Kinesiology*, *19*(2), 232–241. https://doi.org/https://doi.org/10.1016/j.jelekin.2007.08.008

Hunter, S. K., Critchlow, A., & Enoka, R. M. (2005). Muscle endurance is greater for old men compared with strength-matched young men. *Journal of Applied Physiology (Bethesda, Md. : 1985)*, *99*(3), 890–897. https://doi.org/10.1152/japplphysiol.00243.2005

Laidlaw, D. H., Bilodeau, M., & Enoka, R. M. (2000). Steadiness is reduced and motor unit discharge is more variable in old adults. *Muscle & Nerve*, *23*(4), 600–612. https://doi.org/10.1002/(sici)1097-4598(200004)23:4<600::aid-mus20>3.0.co;2-d

Lexell, J. (1995). Human aging, muscle mass, and fiber type composition. J Gerontol A Biol Sci Med Sci. *The Journals of Gerontology. Series A, Biological Sciences and Medical Sciences*, *50 Spec No*, 11–16. https://doi.org/10.1093/gerona/50A.Special_Issue.11

McManus, L., Hu, X., Rymer, W. Z., Suresh, N. L., & Lowery, M. M. (2016). Muscle fatigue increases beta-band coherence between the firing times of simultaneously active motor units in the first dorsal interosseous muscle. *Journal of Neurophysiology*, *115*(6), 2830–2839. https://doi.org/10.1152/jn.00097.2016

Merletti, R., Knaflitz, M., & De Luca, C. J. (1990a). Myoelectric manifestations of fatigue in voluntary and electrically elicited contractions. *Journal of Applied Physiology*, *69*(5), 1810–1820. https://doi.org/10.1152/jappl.1990.69.5.1810

Merletti, R., Knaflitz, M., & De Luca, C. J. (1990b). Myoelectric manifestations of fatigue in

* Indicates the corresponding author: jiangning21@wchscu.cn

voluntary and electrically elicited contractions. *Journal of Applied Physiology (Bethesda, Md. : 1985)*, *69*(5), 1810–1820. https://doi.org/10.1152/jappl.1990.69.5.1810

Mori, D., Sumiil, H., Shiokawa, M., Kunisada, M., Harada, T., Ono, T., & Horiuchi, T. (2016). *Measurement of Low Back Muscle Fatigue and Recovery Time During and After Isometric Endurance Test* (Vol. 489, pp. 297–308). https://doi.org/10.1007/978-3-319-41694-6_31

Moritz, C. T., Barry, B. K., Pascoe, M. A., & Enoka, R. M. (2005). Discharge rate variability influences the variation in force fluctuations across the working range of a hand muscle. *Journal of Neurophysiology*, *93*(5), 2449–2459. https://doi.org/10.1152/jn.01122.2004

Ng, J. K.-F., Parnianpour, M., Richardson, C. A., & Kippers, V. (2003). Effect of fatigue on torque output and electromyographic measures of trunk muscles during isometric axial rotation. *Archives of Physical Medicine and Rehabilitation*, *84*(3), 374–381. https://doi.org/https://doi.org/10.1053/apmr.2003.50008

Sale, D. G. (1987). Influence of exercise and training on motor unit activation. *Exercise and Sport Sciences Reviews*, *15*, 95–151.

Santilli, V., Bernetti, A., Mangone, M., & Paoloni, M. (2014). Clinical definition of sarcopenia. *Clinical Cases in Mineral and Bone Metabolism : The Official Journal of the Italian Society of Osteoporosis, Mineral Metabolism, and Skeletal Diseases*, *11*(3), 177–180.

Tracy, B. L., & Enoka, R. M. (2002). Older adults are less steady during submaximal isometric contractions with the knee extensor muscles. *Journal of Applied Physiology (Bethesda, Md. : 1985)*, *92*(3), 1004–1012. https://doi.org/10.1152/japplphysiol.00954.2001

Tracy, B. L., Maluf, K. S., Stephenson, J. L., Hunter, S. K., & Enoka, R. M. (2005). Variability of motor unit discharge and force fluctuations across a range of muscle forces in older adults. *Muscle & Nerve*, *32*(4), 533–540. https://doi.org/10.1002/mus.20392

Wan, J., Qin, Z., Wang, P., Sun, Y., & Liu, X. (2017). Muscle fatigue: General understanding and treatment. *Experimental & Molecular Medicine*, *49*, e384. https://doi.org/10.1038/emm.2017.194

Wu, R., De Vito, G., Delahunt, E., & Ditroilo, M. (2020). Age-related Changes in Motor Function (I). Mechanical and Neuromuscular Factors. *International Journal of Sports Medicine*, *41*(11), 709–719. https://doi.org/10.1055/a-1144-3408

Yamada, H., Okada, M., Oda, T., Nemoto, S., Shiozaki, T., Kizuka, T., Kuno, S., & Masuda, T. (2000). Effects of aging on EMG variables during fatiguing isometric contractions. *Journal of Human Ergology*, *29*, 7–14.

Yassierli, Nussbaum, M. A., Iridiastadi, H., & Wojcik, L. A. (2007). The influence of age on isometric endurance and fatigue is muscle dependent: a study of shoulder abduction and torso extension. *Ergonomics*, *50*(1), 26–45. https://doi.org/10.1080/00140130600967323

* Indicates the corresponding author: jiangning21@wchscu.cn

Figure Captions

* Indicates the corresponding author: jiangning21@wchscu.cn

* Indicates the corresponding author: jiangning21@wchscu.cn